

# A Comparison of Multirate Robust Track-Following Control Synthesis Techniques for Dual-Stage and Multi-Sensing Servo Systems in Hard Disk Drives

Xinghui Huang, Ryoza Nagamune, and Roberto Horowitz

**Abstract**—This paper presents the design and analysis of multirate robust track-following controllers for a dual-stage servo system with a MEMS microactuator (MA) and an instrumented suspension. Two major categories of controller design methodologies are considered. The first is based on sequential single-input single-output (SISO) design techniques, and includes the sensitivity decoupling (SD) method and the PQ method. High rate inner loop damping control is implemented followed by a low rate outer loop controller. The second category is based on multirate, multi-input multi-output (MIMO) design techniques, including mixed  $H_2/H_\infty$ , mixed  $H_2/\mu$ , and robust  $H_2$  synthesis. In this case, a set of controllers are designed all at once by explicitly considering plant uncertainty and hence robust stability. Comparisons are made between these design techniques in terms of nominal  $H_2$  performance, robust stability, and robust performance. The advantages and disadvantages of each of these methods are discussed, as well as the guidelines for practical implementation.

## I. INTRODUCTION

Since the first hard disk drive (HDD) was invented in the 1950s by IBM, their storage density has been following Moore's law, doubling roughly every 18 months. Current storage density is about 230 giga-bit per square inch, as reported by Hitachi GST [1].

A current goal of the magnetic disk drive industry is to surpass the storage density barrier of 1 terra-bit per square inch. It is expected that the corresponding track density for this storage density will be about 500,000 track-per-inch (TPI), requiring a track mis-registration (TMR) budget of less than 5 nm ( $3\sigma$ ). To achieve this goal, higher control bandwidth is necessary to attain sufficient positioning accuracy. A new class of dual-stage actuators for HDDs has been proposed to overcome this problem: a microactuator (MA) is placed at the end of the suspension and moves the slider/head relative to the suspension tip, allowing increased servo bandwidth [2][3].

However, as servo bandwidth is expanded and the desired TMR budget becomes even smaller, the slider motion due to airflow excited suspension vibration becomes more important as the disk rotation speed increases. Suspension vibration

control schemes using instrumented suspensions along with dual-stage servo systems have thus been proposed. The sensor output from instrumented suspensions can be utilized for vibration damping by the voice coil motor (VCM) [4], or be used for feedforward vibration compensation by the MA [5], or both [6].

Several controller design methods have been proposed for MEMS-based dual-stage servo systems, which can be roughly categorized into two major groups. The first group includes those methodologies that utilize sequential SISO frequency shaping design techniques, such as the sensitivity decoupling (SD) method [7] and the PQ method [8]. These methods are straightforward to implement based on mature SISO design techniques. However, the inherent coupling property of the plant cannot be fully exploited, which usually yields conservative performance with poor robustness properties.

The second group includes multi-variable optimal control design techniques such as  $\mu$ -synthesis [9] and mixed  $H_2/H_\infty$  [6]. With the use of a state-space model, these methods can systematically take into account coupling dynamics and plant uncertainty in the design process. The nominal system's performance can therefore be optimized while still retaining robust stability. The designed controllers usually have a higher order than that of their SISO counterparts. Therefore, a careful tradeoff is necessary when considering computation power, implementation reliability, and achievable performance.

In a MEMS-based dual-stage system with an instrumented suspension, the strain sensor signal and the relative motion information from MA's capacitive sensor can be sampled at a higher rate than that of the position error signal (PES). Multirate sensing and multirate control can then be incorporated into the controller design process. Better performance is therefore expected in track following and vibration attenuation.

This paper presents the design and analysis of robust track-following controllers for a dual-stage servo system with a translational MEMS MA and an instrumented suspension. In Section II, a generalized model is constructed. Section III presents various multirate robust design approaches, including SISO and MIMO techniques. Design and simulation results are presented in Section IV.

This work was supported by the Information Storage Industry Consortium (INSIC), the Swedish Research Council (VR), and the Computer Mechanics Laboratory (CML) of UC Berkeley.

X. Huang is with Seagate Technology, 1251 Waterfront Pl, Pittsburgh, PA 15222, xinghui.huang@seagate.com. R. Nagamune is with the Department of Mathematics, Royal Institute of Technology, Stockholm, Sweden, ryoza@kth.se. R. Horowitz is with the Department of Mechanical Engineering, University of California, Berkeley, CA 94720 horowitz@me.berkeley.edu.



demodulation noise, sensor noises, and A/D quantization noise.

In this paper, the disturbances are modeled as follows. The reference signal,  $r$ , includes track runout and the head motion resulting from all torque disturbances, except the airflow turbulence acting on the two actuators. A 3rd order model is used to characterize its low frequency feature:

$$r(s) = \left( \frac{7.8 \times 10^9}{s^2 + 800s + 2.5 \times 10^5} + \frac{1.2 \times 10^5}{s + 1.9 \times 10^3} \right) w_r(s), \quad (4)$$

where  $w_r$  is a normalized white noise. The RMS value of this runout is about 450 nm in the range of 10 Hz-25 kHz.

The airflow turbulence acting on the two actuators is respectively denoted as  $w_v$  and  $w_m$  for the design purpose. Each suspension mode has an independent disturbance source which is assumed to be white. The  $w_v$ -excited suspension vibration has an RMS value of about 5 nm, and the  $w_m$ -excited MA vibration is about 4 nm. The three signals, PES,  $y_p$  and  $y_m$ , have their corresponding measurement noises with the RMS levels of 1 nm, 0.1 nm and 2 nm, respectively. These noise levels determine how heavily each signal can be utilized so that system performance can be optimized.

### C. Multirate Sensing

In conventional single-stage disk drives, the only feedback signal, PES :=  $r - y_h$ , has a fixed sampling rate that is predetermined by the disk rotation speed and the number of servo sectors per track. The achievable servo bandwidth to about one tenth of this frequency. Further increase of servo bandwidth is also prevented by the presence of suspension resonance modes. With strain sensors instrumented on the suspension and with a secondary microactuator, high frequency suspension vibration may be effectively suppressed and compensated by feeding vibration information to the controller [13] at a higher rate than that of the PES. A multirate controller can then be designed accordingly.

In this paper, we will assume that the PES has a sampling rate of 25 kHz, and both  $y_p$  and  $y_m$  are sampled at 50 kHz. For simplicity, both  $u_v$  and  $u_m$  are updated at the high rate of 50 kHz.

### D. Plant Uncertainty

Plant uncertainty is inherent in all dynamic systems. Hard disk drives are typically fabricated in a huge batch, with each drive having slightly different dynamic response but the same nominal properties. In this section, plant uncertainty is modeled for the dual-stage system so that robust stability can be explicitly considered in control design.

1) *Parametric Uncertainty*: Since the dual-stage model is expressed as a combination of both suspension and MA modes, and each mode is defined by 3 parameters (i.e.,  $A$ ,  $\zeta$ ,  $\omega$ ), it is natural to consider this parametric uncertainty in both control design and performance evaluation. In this paper, the variation range of each parameter relative to its nominal value is specified in Table I.

TABLE I  
PARAMETER VARIATION

	$A$	$\zeta$	$\omega$
$G_V$	$\pm 5\%$	$\pm 20\%$	$\pm 8\%$
$G_M$	$\pm 5\%$	$\pm 20\%$	$\pm 12\%$

2) *Multiplicative Dynamic Uncertainty*: Multiplicative uncertainty can take into account not only unmodeled dynamics but also some effect of parametric uncertainty, a low dimensional  $\Delta$  is therefore adequate for the design purpose. In the dual-stage actuator, two multiplicative uncertainties are assumed for the VCM and MA respectively:

$$\begin{aligned} G_V(s) &= G_{Vnom}(s)(1 + \Delta_V(s)W_V(s)), \\ G_M(s) &= G_{Mnom}(s)(1 + \Delta_M(s)W_M(s)), \end{aligned} \quad (5)$$

where,  $G_{Vnom}$  and  $G_{Mnom}$  are the nominal dynamics of the VCM and MA respectively,  $\|\Delta_V\|_\infty \leq 1$ ,  $\|\Delta_M\|_\infty \leq 1$ , and  $W_V$  and  $W_M$  are the magnitude bounding functions of the two uncertainties, whose magnitude frequency plots are shown in Fig. 4.

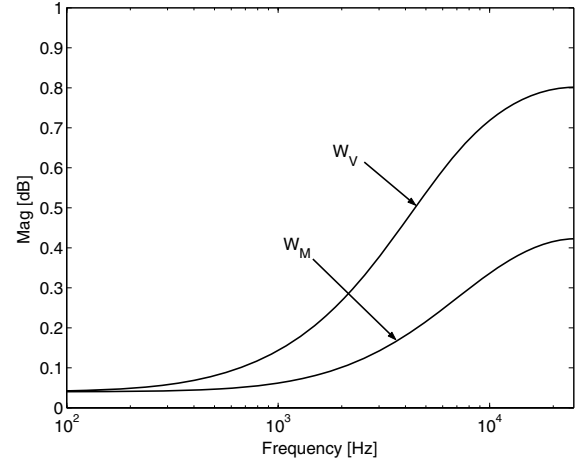


Fig. 4. Multiplicative uncertainties

### E. A Generalized Plant with Multirate Sensing and Control

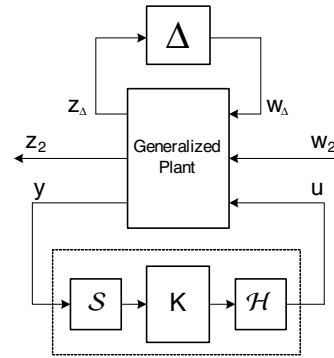


Fig. 5. Multirate sensing and multirate control of the generalized plant

By combining all disturbances, measurement noises, and uncertainty models, we can obtain a generalized plant with

both multirate sensing and multirate control, as shown in Fig. 5. In the figure,  $\Delta$  represents all types of normalized perturbation in block-diagonal form.  $w_2$  includes all types of normalized white disturbances.  $z_2 := [\text{PES } u_v \ u_m]^T$  is the weighted performance output.  $\mathcal{S}$  is the multirate sampler of the plant measurement output  $y := [\text{PES } y_p \ y_m]^T$ . Due to the multirate sampler  $\mathcal{S}$  and hold  $\mathcal{H}$ , the controller  $K$  is also multirate and hence periodically time-varying. The generalized plant has absorbed all frequency shaping filters and weights with all perturbations, disturbances, and performance outputs normalized. Based on this generalized model, various design methods can be applied to design a controller.

### III. ROBUST CONTROLLER DESIGN

#### A. Sequential SISO Designs

In this section, two SISO design approaches are presented: the SD design [7] and the PQ design [14]. Both approaches are realized by a two-step design procedure: a high-rate inner loop damping controller is first implemented, then it's followed by a low-rate track-following controller. This approximation to multi-rate and multi-variable control simplifies the design process and facilitates the use of sequential SISO design techniques at the expense of constraining controller structure, and hence only achieving suboptimal system performance.

1) *Inner Loop Vibration Damping*:  $y_p$  and  $y_m$  are used to design inner loop vibration damping controllers. As previously mentioned, the damping controllers are designed to run at a high rate in order to achieve better attenuation of airflow excited, high-frequency suspension vibrations.

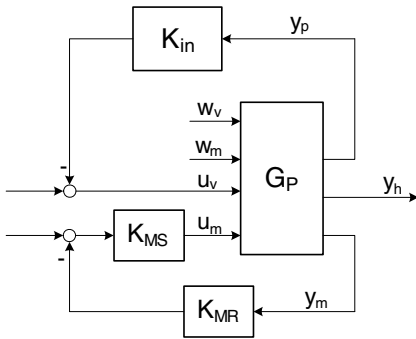


Fig. 6. Minor loop vibration damping and compensation

First, the relative motion signal,  $y_m$ , is used to actively damp the MA resonance mode, as illustrated by the minor loop around the MA in the lower part of Fig. 6, where  $G_P$  is defined in Fig. 2. The two controllers,  $K_{MS}$  and  $K_{MR}$ , are designed by solving a Diophantine equation with a desired closed-loop polynomial  $A_D$ . This polynomial is chosen by the designer based on the tradeoff between airflow excited vibration attenuation and measurement noise amplification [15].

After the minor loop is closed around the MA, a vibration controller  $K_{in}$  is designed using  $y_p$  to provide more damping

for some of the suspension resonance modes. The design of  $K_{in}$  is formulated as a standard LQG problem, in which  $y_v$  is the output to be minimized and  $y_p$  is the feedback signal [13].

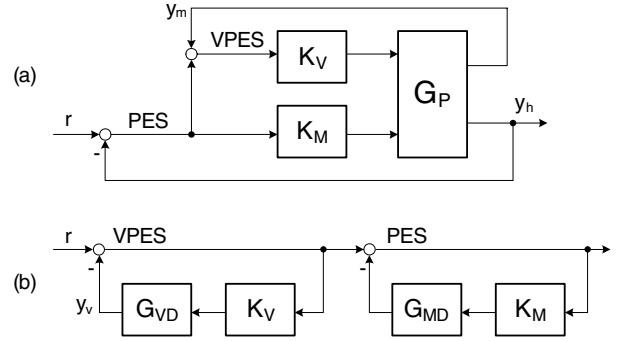


Fig. 7. Sensitivity decoupling design

2) *SD Design*: This approach utilizes the PES and  $y_m$  to generate the position error of the suspension tip relative to the data track center, which will be labelled as VPES:

$$\text{VPES} = \text{PES} + y_m = r - y_v. \quad (6)$$

This signal is then fed to the VCM loop controller  $K_V$ . This scheme is shown in Fig. 7(a), where  $G_{PD}$  is the damped plant as shown in Fig. 6. The closed-loop plant can further be reduced to two sequential loops, as shown in Fig. 7(b). The design of  $K_V$  and  $K_M$  now becomes straightforward: the VCM loop and the MA loop can be designed sequentially using conventional SISO design techniques. The reader is referred to [16] for details of this method.

In order to compare the SD technique with other design approaches, the structure of the complete multirate controller,  $K$  in Fig. 5, of the SD design is given by

$$K_{SD} = \begin{bmatrix} -K_{in} & K_V & K_V \\ 0 & -K_{MS}K_{MR} & K_{MS}K_M \end{bmatrix} \quad (7)$$

with inputs  $[y_s, y_m, \text{PES}]^T$  and outputs  $[u_v, u_m]^T$ . From this we can clearly see the constraints imposed on the controller structure for the ease of applying SISO design techniques. The first column is determined by the inner loop vibration damping using  $y_s$ , and the last two columns are determined by the outer loop controller.

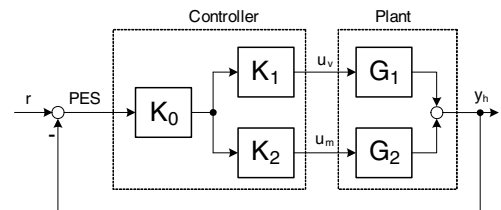


Fig. 8. PQ design

3) *PQ Design*: This approach reduces a control design problem for double-input single-output (DISO) systems to

two sequential SISO designs. The first step of this method addresses the issue of actuator interference as a function of frequency, and the second step allows the use of traditional loop shaping techniques to achieve the desired nominal performance and stability margin. Its scheme is illustrated in Fig. 8, where it is assumed that inner loop damping, such as the one shown in Fig. 6, has been implemented on both the VCM and MA.

To apply the PQ method, we first define

$$G_P(e^{j\omega}) := \frac{G_1(e^{j\omega})}{G_2(e^{j\omega})}, \quad (8)$$

which is the ratio between the two input-output channels of the plant. Subsequently, we design a compensator  $G_Q$  to stabilize the virtual plant  $G_P$  with unity feedback. The phase margin of the open-loop plant  $G_P G_Q$  determines how much the outputs of the two actuators interfere around the handoff frequency. A large phase margin is pursued to ensure that the two actuators work cooperatively. The designed  $G_Q$  is then decomposed into two parts with  $G_Q = K_1/K_2$  such that both  $K_1$  and  $K_2$  are realizable. Finally a compensator  $K_0$  is designed for the SISO plant

$$G_{\text{siso}} := K_1 G_1 + K_2 G_2, \quad (9)$$

to achieve a desired gain crossover frequency and gain and phase margins.

The structure of the complete multirate controller,  $K$  in Fig. 5, for the PD design is given by

$$K_{PQ} = \begin{bmatrix} -K_{\text{in}} & 0 & K_1 K_0 \\ 0 & -K_{MS} K_{MR} & K_{MS} K_2 K_0 \end{bmatrix}. \quad (10)$$

Unlike the sensitivity decoupling design, the PQ method uses only the PES in the outer loop tracking controller. Hence the structure of  $K_{PQ}$  is even more constrained than  $K_{SD}$  in that the entry (2,1) is zero.

## B. MIMO Designs

By exploiting the coupling dynamics inherent in MIMO systems, MIMO robust design methods are expected to achieve better performance than their sequential SISO design counterparts, while still retaining robust stability. In this section, three multirate robust control design approaches are considered: mixed  $H_2/H_\infty$  [17], mixed  $H_2/\mu$ , and robust  $H_2$  synthesis [18].

1) *Mixed  $H_2/H_\infty$  synthesis:* This approach performs nominal  $H_2$  minimization with several  $H_\infty$  bounds on the channels from  $w_\Delta$  to  $z_\Delta$ , so that stability robustness can be explicitly taken into account in the design process. Since the  $H_\infty$  norm is usually not a precise measure for robust stability, especially when the uncertainty  $\Delta$  block has a high dimension, only *multiplicative* uncertainties in the VCM and MA are considered in this design, which restrains the  $\Delta$  block to a 2-by-2 diagonal matrix. Then the problem becomes

$$\min_K \gamma, \text{ subject to } \begin{cases} \|T_{z_2 w_2}(K)\|_2 < \gamma, \\ \|T_{z_V w_V}(K)\|_\infty < \gamma_V, \\ \|T_{z_M w_M}(K)\|_\infty < \gamma_M, \end{cases} \quad (11)$$

where  $(z_V, w_V)$  and  $(z_M, w_M)$  are the I/O channels in the  $\Delta$  block related to the VCM and MA respectively;  $\gamma_V$  and  $\gamma_M$  are bounds selected empirically so that  $\|T_{z_\Delta w_\Delta}(K)\|_\infty < 1$  can finally be satisfied. The reader is referred to [17] for further details.

2) *Mixed  $H_2/\mu$  synthesis:* Unlike mixed  $H_2/H_\infty$  synthesis, mixed  $H_2/\mu$  synthesis minimizes the nominal  $H_2$  norm with a  $\mu$  (structured singular value) bound, since the  $\mu$  bound is a precise measure for robust stability with both parametric and dynamic uncertainty [19]. The design procedure is similar to the  $D$ - $K$  iteration in  $\mu$ -synthesis with the alteration that the  $K$  part is designed by the mixed  $H_2/H_\infty$  optimization procedure rather than an  $H_\infty$  minimization. Therefore, the computation involves a series of optimization steps, and it can be solved via mixed  $H_2/H_\infty$  optimization with proper  $D$ -scaling:

$$\min_{K,D} \gamma, \text{ subject to } \begin{cases} \|T_{z_2 w_2}(K)\|_2 < \gamma, \\ \|DT_{z_\Delta w_\Delta}(K)D^{-1}\|_\infty < 1, \end{cases} \quad (12)$$

where the second inequality represents an upper bound of  $\mu_\Delta(T_{z_\Delta w_\Delta}(K))$ , which guarantees the robust stability of the closed-loop plant. The reader is referred to [19] for more details on  $\mu$  analysis and synthesis. It is noted that the resulting controller order may be large due to the inclusion of dynamic  $D$  and  $D^{-1}$  matrices.

3) *Robust  $H_2$  synthesis:* The previous two approaches can only optimize nominal performance rather than robust performance, and therefore, plant perturbation may degrade track-following performance to an unacceptable extent before the system becomes unstable. The third synthesis approach, robust  $H_2$  synthesis, considers robust (or worst-case), rather than nominal,  $H_2$  performance by taking into account *parametric* uncertainty in the design process. This is achieved by solving

$$\min_K \max_\Delta \|T_{z_2 w_2}(K, \Delta)\|_2. \quad (13)$$

If  $T_{z_2 w_2}(K, \Delta)$  is affine in  $\Delta$ , then this problem can be solved through optimization of a set of matrix inequalities with respect to all vertices of the polyhedron formed by all parametric uncertainties. Since the two decision variables in the matrix inequalities are coupled, which makes the inequalities non-convex, an iteration process is executed to make the optimization step-wise convex by alternatively fixing one of the two variables at each step. This procedure is similar to the  $D$ - $K$  iteration process in  $\mu$  synthesis, and the reader is referred to [20] for more details. The size of the optimization problem increases exponentially with the number of uncertain parameters, and therefore, only a few parametric uncertainties are considered in the design.

Some comments can be made on the three MIMO design approaches. First, all of the three approaches reformulate the multi-objective design problem into the optimization of a set of linear matrix inequalities (LMIs), and which can be solved through convex optimization. Second, the multirate aspect of the problem can be accounted for as follows. An augmented low-rate time-invariant system is constructed from the original high-rate time-varying system with a so-called

$Z$ -cyclic matrix, which contains the periodicity information of the original system. A set of periodically time-varying controllers is then designed all at once, with each controller executed at a certain step within a period. The reader is referred to [18] for more details of the procedure. Third, in accordance with the multirate control design, balanced truncation can be performed on the periodically time-varying full-order controller [21], so that a reduced-order controller is obtained for practical implementation.

#### IV. DESIGN AND SIMULATION RESULTS

The simplified plant used for controller design includes three major modes of the VCM/E-block/suspension assembly and one MA resonance mode. However, the full-order plant model, which includes seven VCM-suspension assembly modes and the MA mode, was used in evaluation and comparison of the designed controllers and closed-loop systems.

Three criteria are checked on the full-order closed-loop systems: robust stability, nominal performance, and worst-case performance. Robust stability is checked in terms of bounded parametric variations defined in Table I. Here, 400 plant samples are formed by randomly picking a set of parameters from within their respective variation ranges. Unstable cases are then counted from the closed-loop systems. If all of these closed-loop systems are stable, then the worst-case performance can be obtained. Here, two performance terms are considered: the RMS values of the PES and the control effort  $u_m$ . The magnitude of  $y_m$  is indirectly constrained to the MA stroke range by minimizing  $u_m$ . The VCM input  $u_v$  is usually very small compared to its working range in the track-following mode. The simulation results are listed in Table II, in which ‘‘Degradation’’ is computed for the worst-case performance w/r to the nominal performance. Controller reduction has been performed before obtaining the final controllers.

Several comparisons can be made between the various design approaches and the following conclusions can be drawn from them.

1) *Robust Stability*: All of the five design methodologies yielded closed-loop systems that are robustly stable under the assumed parametric uncertainty model defined in Table I. For the two SISO techniques, robustness to mode variation is mainly achieved through the incorporation of the inner loop damping of the VCM and MA. For the MIMO designs, stability robustness is considered by imposing auxiliary  $H_\infty$  norm or  $\mu$  bounds, or by considering parametric uncertainty directly.

2) *SISO designs*: As for the two SISO design approaches, the SD method achieves better performance than that of the PQ method, because the relative MA motion,  $y_m$ , is utilized in the design of an outer loop tracking controller for the SD design but not for the PQ design. However, the variance of  $u_m$  is much smaller in the PQ method than in the SD method. This is probably due to the fact that the PQ design methodology explicitly takes actuator interference

into account.

3) *MIMO designs*: The mixed  $H_2/\mu$  approach achieved the best nominal and worst case performance in all three MIMO techniques. This is attributed to the precise characterization of robust stability criterion through  $\mu$ , which makes the controller less conservative and be fully exploited. The robust  $H_2$  design achieves moderate performance with the smallest performance degradation. This is mainly due to the explicit consideration of worst-case performance in the design process. Both of the two methods yielded controllers that perform better than the mixed  $H_2/H_\infty$  design, indicating the conservativeness of  $H_\infty$  norm bounds for stability robustness.

4) *SISO design vs. MIMO design*: It can be clearly seen that the MIMO designs always perform better than their sequential SISO counterparts, not only in terms of nominal performance, but also of worst-case performance. Performance degradation due to parameter variations also shows the same trend: it increases at a smaller rate for MIMO designs than for SISO designs.

It is also observed that the control input effort at the MA,  $u_m$ , is not necessarily larger in MIMO designs than in SISO designs. This implies that MIMO designs achieve small tracking errors by optimizing their controllers rather than by putting more control effort into the system.

5) *Multi-sensing*: The effect of multi-sensing is also checked by comparing different sensing schemes. In Table II, the robust  $H_2$  results are labelled by a 3-element vector indicating the availability of the three outputs [PES  $y_p$   $y_m$ ]. A value of 1 means that the corresponding signal was used in the control structure, while a 0 indicated that the signal was unused. A comparison of the four cases of robust  $H_2$  shows that the use of either  $y_m$  and  $y_p$  can improve system performance significantly, while using both signals can achieve the best nominal performance with the smallest performance degradation. The use of  $y_m$  makes the MA more robust to its mode uncertainty, and also makes it possible to optimally distribute control effort between the two actuators. However, a dedicated vibration sensor can provide suspension vibration information at a higher signal-to-noise ratio and hence is necessary when approaching the extremely stringent target, 500k TPI.

6) *Controller order*: Controller reduction was conducted on all three MIMO controllers for practical implementation. It is observed that since these controllers are MIMO and dynamically coupled, they may be more sensitive to quantization error than their sequential SISO counterparts. It also be noted that a set of controllers are designed all at once. Therefore, more memory is needed for storing these controllers parameters.

#### V. CONCLUSION

In this paper, we have presented the system modelling, design, and comparison of several multirate robust track-following controllers for a dual-stage servo system that

TABLE II

PERFORMANCE COMPARISON BETWEEN CONTROL DESIGNS.

Unstable cases are counted based on 400 perturbed plants. ‘Degradation’ denotes the ratio of worst-case over nominal performance. The 3-element vectors for robust  $H_2$  indicate the availability of the three outputs [PES  $y_p$   $y_m$ ].

Design Approach	Unstables (/400)	PES (nm)			$u_m$ (mV)			Controller Order
		Nominal	W.C.	Degradation	Nominal	W.C.	Degradation	
PQ method	0	7.75	10.00	129 %	205	234	114 %	6
SD method	0	7.11	8.35	117 %	277	316	114 %	6
Mixed $H_2/H_\infty$	0	6.57	7.82	119 %	201	216	108 %	8
Mixed $H_2/\mu$	0	5.31	5.88	111 %	261	298	114 %	8
Robust $H_2$ [1 1 1]	0	5.93	6.47	109 %	275	310	113 %	9
Robust $H_2$ [1 0 1]	0	5.96	7.10	118 %	308	388	126 %	10
Robust $H_2$ [1 1 0]	0	6.09	7.97	131 %	239	309	129 %	10
Robust $H_2$ [1 0 0]	0	7.66	9.45	123 %	278	399	144 %	10

utilizes a MEMS microactuator and an instrumented suspension. A complete plant model, including nominal dynamics, sensing schemes, disturbances, and plant uncertainties, was developed. Two SISO design approaches, the PQ design and the SD design, and three multirate robust MIMO design approaches, mixed  $H_2/H_\infty$ , mixed  $H_2/\mu$  and robust  $H_2$  synthesis, were considered.

Design and simulation results showed that the robust MIMO design approaches generally achieve better nominal and worst-case performance than their sequential SISO design approach counterparts. These advantages were achieved by optimizing the  $H_2$  performance of the control system, while considering robust stability explicitly, and also by making the controller multirate in a strict sense. On the other hand, the SISO design approaches are straightforward to use and easy to implement.

## REFERENCES

- [1] HGST, ‘‘Perpendicular recording,’’ [http://www.hitachigst.com/hdd/research/recording\\_head/pr/index.html](http://www.hitachigst.com/hdd/research/recording_head/pr/index.html), 2005.
- [2] T. Hirano, M. White, H. Yang, K. Scott, S. Pattanaik, S. Arya, and F.-Y. Huang, ‘‘A moving-slider MEMS actuator for high-bandwidth HDD tracking,’’ in *Proc. of Intermag*, vol. 3, Anaheim, CA, 2003, pp. 2535–2540.
- [3] K. Oldham, S. Kon, and R. Horowitz, ‘‘Fabrication and optimal strain sensor placement in an instrumented disk drive suspension for vibration suppression,’’ in *Proc. American Control Conf.*, 2004, pp. 1855–1860.
- [4] Y. Huang, M. Banther, P. D. Mathur, and W. Messner, ‘‘Design and analysis of a high bandwidth disk drive servo system using an instrumented suspension,’’ *IEEE/ASME Trans. Mechatronics*, vol. 4, no. 2, pp. 196–206, 1999.
- [5] Y. Li and R. Horowitz, ‘‘Active vibration control of a PZT actuated suspension in hard disk drives,’’ in *Proc. American Control Conf.*, 2002, pp. 1366–1371.
- [6] X. Huang, R. Nagamune, R. Horowitz, and Y. Li, ‘‘Design and analysis of a dual-stage disk drive servo system using an instrumented suspension,’’ in *Proc. American Control Conf.*, 2004, pp. 535–540.
- [7] Y. Li and R. Horowitz, ‘‘Mechatronics of electrostatic microactuators for computer disk drive dual-stage servo systems,’’ *IEEE/ASME Trans. Mechatronics*, vol. 6, no. 2, pp. 111–121, 2001.
- [8] S. J. Schroeck and W. C. Messner, ‘‘On controller design for linear time-invariant dual-input single-output systems,’’ in *Proc. American Control Conf.*, 1999, pp. 4122–4126.
- [9] D. Hernandez, S.-S. Park, R. Horowitz, and A. K. Packard, ‘‘Dual-stage track-following servo design for hard disk drives,’’ in *Proc. American Control Conf.*, 1999, pp. 4188–4121.
- [10] R. Ehrlich and D. Curran, ‘‘Major HDD TMR sources and projected scaling with TPI,’’ *IEEE Trans. Magnetism*, vol. 35, no. 2, pp. 885–891, 1999.
- [11] L. Guo, H. S. Lee, A. Hudson, and S.-H. Chen, ‘‘A comprehensive time-domain simulation for HDD TPI prediction and mechanical/servo enhancement,’’ *IEEE Trans. Magnetism*, vol. 35, no. 2, pp. 879–884, 1999.
- [12] L. Guo and Y.-J. D. Chen, ‘‘Disk flutter and its impact on HDD servo performance,’’ *IEEE Trans. Magnetism*, vol. 37, no. 2, pp. 866–870, 2001.
- [13] Y. Li, F. Marcassa, R. Horowitz, R. Oboe, and R. Evans, ‘‘Track-following control with active vibration damping of a PZT-actuated suspension dual-stage servo system,’’ in *Proc. American Control Conf.*, 2003, pp. 2553–2559.
- [14] W. Messner and R. Ehrlich, ‘‘A tutorial on controls for disk drives,’’ in *Proc. American Control Conf.*, 2001, pp. 408–420.
- [15] M. T. White and T. Hirano, ‘‘Use of relative position signal for microactuators in hard disk drives,’’ in *Proc. of American Control Conf.*, 2003, pp. 2535–2540.
- [16] Y. Li and R. Horowitz, ‘‘Active suspension vibration control with dual-stage actuators in hard disk drives,’’ in *Proc. American Control Conf.*, 2001, pp. 2786–2791.
- [17] X. Huang and R. Horowitz, ‘‘Robust controller design of a dual-stage disk drive servo system with an instrumented suspension,’’ *IEEE Trans. Magnetism*, vol. 8, no. 5, pp. 194–200, 2005.
- [18] R. Nagamune, X. Huang, and R. Horowitz, ‘‘Multirate track-following control with robust stability for dual-stage multi-sensing servo systems in HDDs,’’ in *Proc. IEEE Conf. on Decision and Control*, Dec 2005.
- [19] G. J. Balas, J. C. Doyle, K. Glover, A. Packard, and R. Smith,  *$\mu$ -Analysis and Synthesis Toolbox for use with MATLAB*. MUSYN Inc. and The MathWorks, Inc., USA, 1995.
- [20] R. Nagamune, X. Huang, and R. Horowitz, ‘‘Robust  $H_2$  synthesis for dual-stage multi-sensing track-following servo systems in HDDs,’’ in *Proc. American Control Conf.*, 2006.
- [21] A. Varga, ‘‘Balanced truncation model reduction of periodic systems,’’ in *Proc. 39th IEEE Conf. on Decision and Control*, 2000, pp. 2379–2384.